JACS
JOURNAL OF THE AMERICAN CHEMICAL SOCIETY

COMMUNICATION

pubs.acs.org/JACS

Enhanced Catalytic Activity on Titanosilicate Molecular Sieves Controlled by Cation−π Interactions

Yasutaka Kuwahara,[†] Kazuto Nishizawa,[†] Takahito Nakajima,[‡] Takashi Kamegawa,[†] Kohsuke Mori,[†] and Hiromi Yamashita*[,†]

[†]Division of Materials and Manufacturing Science, Graduate School of Engineering, Osaka University, 2-1 Yamada-oka, Suita, Osaka, Japan

[‡]Computational Molecular Science Research Team, Advanced Institute for Computational Science, RIKEN, 7-1-26 minatojima-minami, Cyuo, Kobe, Hyogo, Japan

Supporting Information

ABSTRACT: A new class of heterogeneous catalytic systems utilizing cation−guest interactions was designed based on microporous titanosilicate molecular sieves. Introducing heavier alkali metal cations on ion-exchange sites of the framework resulted in a significant enhancement of the catalytic activity for oxidation of cyclohexene and styrene, whereas such an enhancement was not observed in oxidation of cyclohexane without π systems. Distinct relationships between the catalytic activities and intermolecular interaction energies which were determined by IR spectroscopic and computational approaches clearly evidenced the predominance of the cation−π interaction in this catalytic system.

Molecular sieve materials bearing multiple function sites can offer immense possibilities for the design of catalytic systems with specific properties. Among this material family, titanosilicate molecular sieves, exemplified by TS-1[1] and Ti-MCM-41,[2] have been well-known to be efficient catalysts for the oxidation of a variety range of hydrocarbons using H_2O_2.[3] This is primarily because of high selectivity in products originating from tetrahedrally coordinated Ti species in the silica matrix, strictly ordered micro/meso porous structures and relatively hydrophobic nature of the surface. In such catalytic systems, precise control of microenvironment, such as crystal architecture, hydrophobicity/organophilicity, polarity and electric charge density of the surface, is one of the key subjects for achieving high catalytic-efficiency because they significantly influence molecular dynamics and physicochemical properties of guest molecules.[4−7] Much effort has been directed so far toward direct/postsynthetic silylation of their surfaces using organosilanes,[8] otherwise, grafting of organotitanate species substituting surface silanols,[9] which offer improved catalytic activities by creating hydrophobic surfaces. Another possible approach is the employment of specific intermolecular interactions between the solid surface and the target organic molecules.

In this communication, we report a new approach which utilizes a cation−π interaction for improving catalytic activity in molecular sieve-based catalytic systems (Scheme 1). Cation−π interaction, an intermolecular interaction between the face of a π system and an adjacent cation,[10] has been recognized as a powerful conformation-controlling tool in synthetic organic chemistry (e.g., use of Na^+ cations in Na−Y zeolite as conformational recognition sites for chemoselective hydroperoxidation of alkenylarenes[11] or as activation sites for aldehyde derivatives[12]) due to its strength several times greater than other interactions, such as hydrogen bonding and van der Waals force. However, little is known about its application to heterogeneous catalytic systems.

To examine the effect of alkali cations on catalysis, we prepared a series of alkali metal cation functionalized titanosilicate molecular sieves, M^+@[Al,Ti]-ZSM-5 ($M^+ = Li^+$, Na^+, K^+, Rb^+, and Cs^+), from calcined [Al,Ti]-ZSM-5[1] by repeated ion-exchange procedures (Si/Al and Si/Ti molar ratios were determined to be 72 and 139, respectively). X-ray diffraction and N_2 adsorption identified microporous structures with MFI topology having large surface area ($S_{BET} \sim 460\ m^2/g$) (Figure S1 and S2, Supporting Information [SI]). By means of FT-IR,[13] UV−vis, and Ti K-edge XAFS measurements,[14] the coordination geometries of Al and Ti atoms were confirmed to be both typical of tetrahedral coordination, indicating the isomorphorous substitution of these atoms within the silica matrix (Figure S3−S5,SI). On the basis of elemental analysis, the ion-exchanged rates of cations exceeded 95% in any cases, and no appreciable loss in crystallinity was observed even after the repeated ion-exchange procedures.

To demonstrate the cation−guest interactions, we examined catalytic activity of the prepared samples using cyclohexene epoxidation with H_2O_2 as a test reaction (Table 1). An Al-free titanosilicate (TS-1) generally favored for this use because of its hydrophobic nature of the surface compared with Al-containing titanosiliate molecular sieves[5] afforded TON = 38 and 72.2% cyclohexene oxide selectivity; however, a series of M^+-functionalized materials showed superior cyclohexene conversion to TS-1. The TON increased as the size of the alkali metal cations increased, viz. $Li^+ < Na^+ < K^+ < Rb^+ < Cs^+$, and Cs^+@[Al,Ti]-ZSM-5 provided the highest activity (TON = 135), which was 3.6 times higher than that of TS-1, with improved epoxide selectivity (82.9%). Meanwhile, H^+@[Al,Ti]-ZSM-5 resulted in quite poor selectivity of epoxide (19.7%) due to its acidic nature. The improved epoxide selectivity over M^+@[Al,Ti]-ZSM-5 is well consistent with the previous results by Goa et al. which proved that ion-exchange with quaternary ammonium cations

Received: June 20, 2011
Published: July 22, 2011

decreases density of acid sites and retards the formation of byproducts.[15] Furthermore, H_2O_2 conversion correspondingly increases by employing larger alkali metal cations, verifying improved catalytic efficiency. Such an enhancement in catalytic activity was not observed with different ionic state of Cs atoms; neither using Cs-impregnated TS-1 nor direct addition of equivalent amount of Cs_2CO_3 in the reaction solution with TS-1 made any significant contribution to the TON (see Table S2).[16] These catalytic results unambiguously indicate that Cs^+ atoms cationically immobilized on ion-exchange sites affect the conversion rate, serving as adsorption sites not as cocatalysts.

Khouw et al. and Tatsumi et al., who examined the effect of Na^+ and K^+ cations as impurities during the synthesis, have commonly reported the negative contributions of alkali cations to the catalytic activity and selectivity in the oxidation of aliphatic olefins. This can be attributed to the high polarity of alkali metal cations located adjacent to the Ti atoms in the form of ≡Si−O^-M^+ (M^+ = Na^+, K^+ etc.).[17,18] In order to clarify the role of alkali metal cations in our case, cyclohexene adsorption followed by FT-IR measurement was conducted. Among several distinguishable bands observed in the C−H stretching vibration region,[19] a band assignable to stretching mode of olefinic =CH− bond was observed at around 3028 cm^{-1} on TS-1.[20] A shift of this band toward lower wavenumbers was observed by introducing and continuously changing the alkali metal cations from Cs^+ to Li^+ (Figure S6, SI), suggesting an interaction between cyclohexene molecules and the alkali metal cations. A clear inverse correlation can be found between the TON and the IR peak position corresponding to the olefinic bond of the chemisorbed cyclohexene (Figure 1A). This result can be explained in terms of changes in the interaction energy of the alkali cations; lighter alkali cations located inside of the micropore channels may act as stronger adsorption sites, giving rise to a stronger attractive force toward electron-rich olefin double bonds, than heavier alkali cations. On the contrary, neither any appreciable enhancement in catalytic activity nor any band shift in IR spectra was observed in the case of cyclohexane, a saturated cyclic hydrocarbon with molecular structure similar to that of cyclohexene (for catalytic results, see Table S3 in SI).[21]

Above tendency is also corroborated by atomistic consideration based on Sanderson's electronegativity, which is well-accepted as a criterion to determine the equalized electronegativity of zeolite frameworks.[22] We can identify closely similar relationship between the TON in the cyclohexene epoxidation and the electronegativity of the unit cell of the M^+@[Al,Ti]-ZSM-5 (Figure 1B), i.e. higher catalytic activity can be obtained as the attracting force toward electrons is weakened. These experimental results evidence the predominance of the cation−guest interaction in this catalytic system.

To clarify the intricate cation−guest interactions at the molecular level, ab initio molecular orbital calculations were carried out adopting three-component supramolecular systems comprised of an organic adsorbate, a relaxed cluster model of zeolite framework, and an alkali metal cation.[23,24] The conformational geometry of the cyclohexene molecule fully optimized with a Si(1)Al(1) cluster model and a Cs^+ cation is schematically illustrated in Figure 2A. In the MP2 optimized conformations, the olefin double bond of cyclohexene molecule always faced toward the alkali metal cation, which is electrostatically stabilized in the vicinity of the Si(1)Al(1) cluster, and no significant overlapping between the orbitals of cyclohexene molecules and cations was observed, suggesting that the cyclohexene molecules are stabilized on the alkali cations by electrostatic interactions. The adsorption energy between the cyclohexene molecule and the alkali metal cation, ΔH_{ads}, obtained from the calculated total energy of the supramolecular systems linearly decreased by

Scheme 1. Molecular Dynamics of Cyclohexene Molecules within the Micropores of Alkali Metal Cation Functionalized [Al,Ti]-ZSM-5 Molecular Sieve

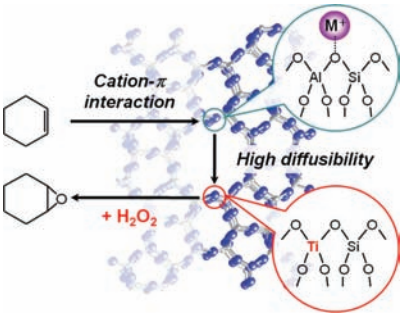

Table 1. Textual Properties and Results in Cyclohexene Epoxidation of Alkali Metal Cation-Functionalized [Al,Ti]-ZSM-5

				N_2 ads.		cyclohexene epoxidation [e]			
sample	unit cell composition[a]	ionic radii of alkali cation (Å)	Sanderson's electronegativity[b]	S_{BET}[c] (m^2/g)	V_{micro}[d] (cm^3/g)	TON[f]	S_{epox}[g] (%)	H_2O_2 conv. (%)	H_2O_2 eff.[h] (%)
TS-1	$Ti_{0.7}Si_{95.3}O_{192}$	–	4.221	453	0.190	38	72.2	10.0	22.2
Li^+@[Al,Ti]-ZSM-5	$Li_{1.26}H_{0.06}Al_{1.32}Ti_{0.68}Si_{94}O_{192}$	0.68	4.212	463	0.189	45	76.5	5.3	50.0
Na^+@[Al,Ti]-ZSM-5	$Na_{1.32}Al_{1.32}Ti_{0.68}Si_{94}O_{192}$	0.97	4.210	455	0.187	69	93.6	7.6	53.6
K^+@[Al,Ti]-ZSM-5	$K_{1.32}Al_{1.32}Ti_{0.68}Si_{94}O_{192}$	1.33	4.200	452	0.184	93	93.2	9.7	53.1
Rb^+@[Al,Ti]-ZSM-5	$Rb_{1.30}H_{0.02}Al_{1.32}Ti_{0.68}Si_{94}O_{192}$	1.55	4.197	435	0.180	109	83.4	12.6	50.6
Cs^+@[Al,Ti]-ZSM-5	$Cs_{1.30}H_{0.02}Al_{1.32}Ti_{0.68}Si_{94}O_{192}$	1.70	4.193	431	0.175	135	82.9	15.5	51.0

[a] Determined by ICP analysis. [b] Calculated according to the equation $(S_M{}^p\, S_H{}^q\, S_{Al}{}^r\, S_{Ti}{}^t\, S_{Si}{}^u\, S_O{}^v)^{1/(p+q+r+t+u+v)}$, where S_M, S_H, S_{Al}, S_{Ti}, S_{Si}, and S_O represent the Sanderson's electronegativities of the alkali metal cation, hydrogen, aluminum, titanium, silicon, and oxygen, respectively, and p, q, r, t, u, and v represent the number of the corresponding element in a unit cell, respectively.[22] [c] Calculated from the adsorption branch of the N_2 isotherms by BET (Brunauer−Emmett−Teller) method. [d] Determined by α_s-plot. [e] Reaction conditions: catalyst (50 mg), cyclohexene (10 mmol), H_2O_2 (30% aqueous solution, 10 mmol), acetonitrile (10 mL), 60 °C, 4 h. [f] TON = [moles of cyclohexene converted]/[moles of Ti]. [g] Selectivity of epoxide. [h] Calculated by [moles of cyclohexene converted]/[moles of H_2O_2 consumed] × 100.

dx.doi.org/10.1021/ja205699d |J. Am. Chem. Soc. 2011, 133, 12462–12465

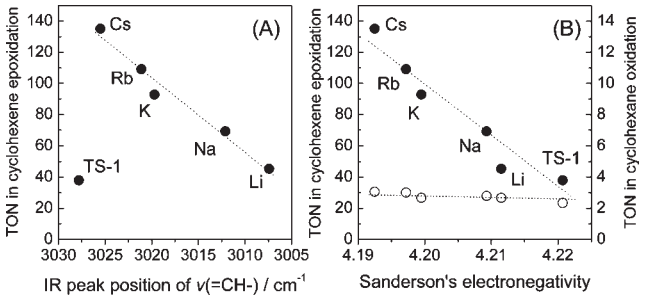

Figure 1. (A) Correlation between TON in cyclohexene epoxidation and IR peak position corresponding to the olefinic =CH− bond of cyclohexene chemisorbed on M^+@[Al,Ti]-ZSM-5 and (B) Correlation between TON in oxidation reactions and Sanderson's electronegativity (●: cyclohexene, ○: cyclohexane).

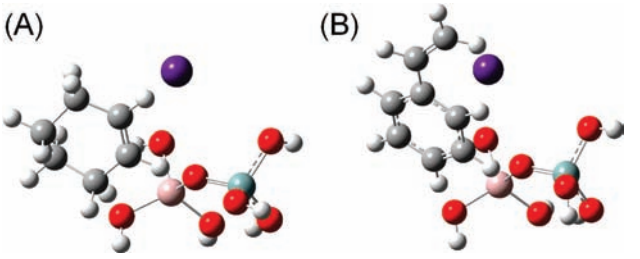

Figure 2. Optimized conformational geometries of supramolecular systems comprising adsorbate molecules ((A) cyclohexene and (B) styrene), Cs^+ cations, and Si(1)Al(1) model clusters. (white: H, gray: C, red: O, pink: Al, light blue: Si, and purple: Cs).

varying the alkali cations from Li^+ to Cs^+ (Figure 3A), theoretically proving that the larger alkali cation has weaker electrostatic interaction between cyclohexene molecule. Furthermore, the TON in the cyclohexene epoxidation plotted against the obtained ΔH_{ads} values afforded a similar correlation to that observed in Figure 1 (Figure 3B). On the other hand, calculations using cyclohexane as an adsorbate demonstrated that adsorption energy of cyclohexane is independent of the kind of alkali metal cations. These results well agree with the experimental results.

On the basis of the experimental and computational results, we can attribute the enhancement of catalytic activity to weak cation−π interactions between heavier alkali metal cations and adjacent olefin molecules which improves the diffusibility of olefin molecules within the micropores, where the heavier alkali metal cations work as reversible adsorption sites; contrarily, lighter alkali metal cations hinder the diffusion due to a strong cation−π interaction.

In the case of styrene oxidation (Figure 4 B),[25] the influence on catalytic activity was less pronounced compared with the case of cyclohexene epoxidation, although the TON continuously increased with increasing the size of alkali metal cations (TON: 38 for TS-1 and 55 for Cs^+@[Al,Ti]-ZSM-5, see also Table S4, SI). This is primarily because products are also under the influence of cation−π interaction. As shown in Figure 2B, the optimized conformational geometry of styrene molecule visually suggests the interaction between a Cs^+ cation and the aromatic ring. The $-\Delta H_{ads}$ value between Cs^+ and styrene calculated under the most stable conformational geometry was 12.94 kcal/mol, which is quite larger than that between Cs^+ and cyclohexene,

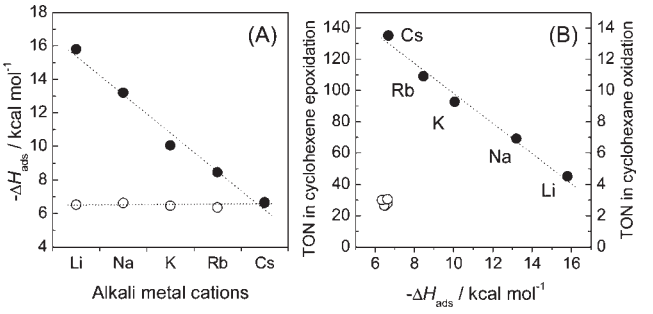

Figure 3. (A) Adsorption energy between the adsorbate molecules (●: cyclohexene, ○: cyclohexane) and the alkali metal cations stabilized on Si(1)Al(1) model clusters, $-\Delta H_{ads}$. (B) Correlation between TON in oxidation reactions and $-\Delta H_{ads}$ (●: cyclohexene, ○: cyclohexane).

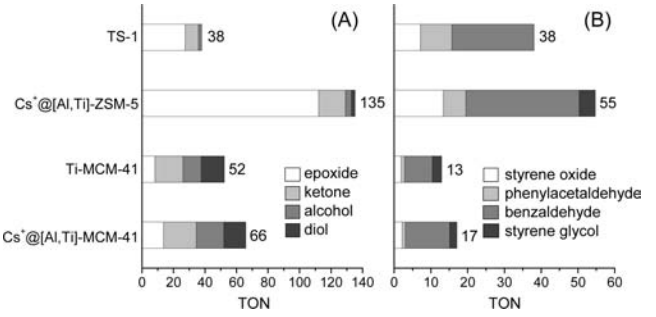

Figure 4. TON for the oxidation of (A) cyclohexene and (B) styrene with H_2O_2 over various titanosilicate molecular sieves. Reaction conditions are described in the footnote. TON = [moles of olefin converted]/[moles of Ti].

6.68 kcal/mol. It is presumable that the interaction between π-conjugated systems of aromatic rings and alkali cations retards the diffusion of styrene and byproduct molecules, which results in slight increase of the catalytic activity.

It is also worth mentioning that such a significant enhancement was not observed in the case of mesoporous silica-based materials, Cs^+@[Al,Ti]-MCM-41,[26] with diameter of 2.7 nm which is ca. 5 times larger than that of ZSM-5 zeolite (the widest diameter of 5.6 Å). Oxidation of cyclohexene with H_2O_2 gave TON = 66 for Cs^+@[Al,Ti]-MCM-41, which is slightly higher than that of Ti-MCM-41 (TON = 52), and oxidation of styrene resulted in similar results (Figure 4A,B, see also Table S5 [SI] for details). These comparative studies imply that the cation−π interaction predominantly works only within the restricted microspaces of zeolites, where olefin molecules are forced to be located adjacent to the cation sites.

In summary, we can conclude that heavier alkali cations are capable of improving diffusional properties of olefin molecules acting as reversible adsorption sites via a weak cation−π interaction, and thus the catalytic activity is enhanced. The theoretical concept of this enhancement is in marked contrast to the previous principles in titanosilicate molecular sieve catalysts: Al and the corresponding exchangeable cation sites provide hydrophilic environment, where water and polar solvents are strongly adsorbed, and the organic substrates have a limited access to the active sites.[5,17,18] This study demonstrated that utilization of cation−guest interaction provides a method for achieving high catalytic efficiency in particular catalytic reactions. We expect that

the insight obtained in this study can be further extendible to the other molecular sieve-based catalytic systems bearing different catalytically active centers.

■ ASSOCIATED CONTENT

Supporting Information. Detailed information on the material synthesis, activity characterization, XRD, sorption, IR, and XAFS studies. This material is available free of charge via the Internet at http://pubs.acs.org.

■ AUTHOR INFORMATION

Corresponding Author
yamashita@mat.eng.osaka-u.ac.jp

■ ACKNOWLEDGMENT

This work is supported by the Grant-in-Aid for Scientific Research (KAKENHI) in Priority Area "Molecular Nano Dynamics" from Ministry of Education, Culture, Sports, Science and Technology of Japan (No. 23360356). Y.K. thanks the JSPS research Fellowships for Young Scientists.

■ REFERENCES

(1) (a) Clerici, M. G.; Bellusi, G.; Romano, U. *J. Catal.* **1991**, *129*, 159–167. (b) Bellussi, G.; Rigutto, M. S. *Stud. Surf. Sci. Catal.* **2001**, *137*, 911–955. (c) Fan, W.; Duan, R. G.; Yokoi, T.; Wu, P.; Kubota, Y.; Tatsumi, T. *J. Am. Chem. Soc.* **2008**, *130*, 10150–10164.

(2) (a) Corma, A.; Navarro, M. T.; Pérez-Pariente, J. *J. Chem. Soc., Chem. Commun.* **1994**, 147–148. (b) Blasco, T.; Corma, A.; Navarro, M. T.; Pérez-Pariente, J. *J. Catal.* **1995**, *156*, 65–74. (c) Corma, A. *Chem. Rev.* **1997**, *97*, 2373–2419.

(3) (a) Pinnavaia, T. J.; Zhang, W. *Stud. Surf. Sci. Catal.* **1998**, *117*, 23–36. (b) Corma, A.; Navarro, M. T.; Pérez-Pariente, J.; Sánchez, F. *Stud. Surf. Sci. Catal.* **1994**, *84*, 69–75. (c) Wu, P.; Tatsumi, T. *Catal. Surv. Asia* **2004**, *8*, 137–148. (d) Huybrechts, D. R. C.; De Bruycker, L.; Jacobs, P. A. *Nature* **1990**, *345*, 240–242. (e) Balducci, L.; Bianchi, D.; Bortolo, R.; D'Aloisio, R.; Ricci, M.; Tassinari, R.; Ungarelli, R. *Angew. Chem., Int. Ed.* **2003**, *42*, 4937–4940.

(4) (a) Xiao, F. S.; Han, Y.; Yu, Y.; Meng, X.; Yang, M.; Wu, S. *J. Am. Chem. Soc.* **2002**, *124*, 888–889. (b) Yokoi, T.; Karouji, T.; Ohta, S.; Kondo, J. N.; Tatsumi, T. *Chem. Mater.* **2010**, *22*, 3900–3908.

(5) (a) Camblor, M. A.; Corma, A.; Esteve, P.; Martínez, A.; Valencia, S. *Chem. Commun.* **1997**, 795–796. (b) Blasco, T.; Camblor, M. A.; Corma, A.; Esteve, P.; Guil, J. M.; Martínez, A.; Perdigón-Melón, J. A.; Valencia, S. *J. Phys. Chem. B* **1998**, *102*, 75–88.

(6) (a) Ramamurthy, V.; Corbin, D. R.; Johnston, L. J. *J. Am. Chem. Soc.* **1992**, *114*, 3870–3882. (b) Ramamurthy, V.; Caspar, J. V.; Eaton, D. F.; Kuo, E. W.; Corbin, D. R. *J. Am. Chem. Soc.* **1992**, *114*, 3882–3892.

(7) (a) Taira, N.; Saitoh, M.; Hashimoto, S.; Moon, H. R.; Yoon, K. B. *Photochem. Photobiol. Sci.* **2006**, *5*, 822–827. (b) Mori, K.; Kagohara, K.; Yamashita, H. *J. Phys. Chem. C* **2008**, *112*, 2593–2600.

(8) For direct-synthesis with organosilanes, see: (a) Corma, A.; Jordá, J. L.; Navarro, M. T.; Rey, F. *Chem. Commun.* **1998**, 1899–1900. (b) Igarashi, N.; Kidani, S.; Ahemaito, R.; Hashimoto, K.; Tatsumi, T. *Microporous Mesoporous Mater.* **2005**, *81*, 97–105. For postsynthetic trimethyl silylation, see:(c) Corma, A.; Domine, M.; Gaona, J. A.; Jordá, J. L.; Navarro, M. T.; Rey, F.; Pérez-Pariente, J.; Tsuji, J.; McCulloch, B.; Nemeth, L. T. *Chem. Commun.* **1998**, 2211–2212. (d) Tatsumi, T.; Koyano, K. A.; Igarashi, N. *Chem. Commun.* **1998**, 325–326. For silylation using triethoxyfluorosilane, see: (e) Sonoda, J.; Kamegawa, T.; Kuwahara, Y.; Mori, K.; Yamashita, H. *Bull. Chem. Soc. Jpn.* **2010**, *83*, 592–594.

(9) (a) Maschmeyer, T.; Rey, F.; Sankar, G.; Thomas, J. M. *Nature* **1995**, *378*, 159–162. (b) Oldroyd, R. D.; Thomas, J. M.; Maschmeyer, T.; MacFaul, P. A.; Snelgrove, D. W.; Ingold, K. U.; Wayner, D. D. M. *Angew. Chem., Int. Ed.* **1997**, *35*, 2787–2790. (c) Jarupatrakorn, J.; Tilley, T. D. *J. Am. Chem. Soc.* **2002**, *124*, 8380–8388.

(10) Ma, J. C.; Dougherty, D. A. *Chem. Rev.* **1997**, *97*, 1303–1324.

(11) (a) Stratakis, M.; Froudakis, G. *Org. Lett.* **2000**, *2*, 1369–1372. (b) Stratakis, M.; Rabalakos, C.; Mpourmpakis, G.; Froudakis, G. E. *J. Org. Chem.* **2003**, *68*, 2839–2843. (c) Stratakis, M.; Kalaitzakis, D.; Stavroulakis, D.; Kosmas, G.; Tsangarakis, C. *Org. Lett.* **2003**, *5*, 3471–3474.

(12) (a) Okachi, T.; Fujimoto, K.; Onaka, M. *Org. Lett.* **2002**, *4*, 1667–1669. (b) Okachi, T.; Onaka, M. *J. Am. Chem. Soc.* **2004**, *126*, 2306–2307. (c) Imachi, S.; Onaka, M. *Chem. Lett.* **2005**, *34*, 708–709.

(13) Ali, M. A.; Brisdon, B.; Thomas, W. J. *Appl. Catal., A* **2003**, *252*, 149–162.

(14) Thomas, J. M.; Sankar, G. *Acc. Chem. Res.* **2001**, *34*, 571–581.

(15) (a) Goa, Y.; Wu, P.; Tatsumi, T. *Chem. Commun.* **2001**, 1714 1715. (b) Goa, Y.; Wu, P.; Tatsumi, T. *J. Phys. Chem. B* **2004**, *108*, 8401–8411.

(16) Cs-impregnated TS-1 (Si/Cs = 72) gave TON = 58 and 88.2% epoxide selectivity and direct addition of equivalent Cs_2CO_3 in the reaction solution with TS-1 resulted in TON = 31 and >99% selectivity. In all cases, the incorporated amount of Cs^+ cation, varied from 1.9−4.0 mols per Ti atom, did not strongly influence the TON under our reaction conditions.

(17) Khouw, C. B.; Davis, M. E. *J. Catal.* **1995**, *151*, 77–86.

(18) Tatsumi, T.; Koyano, K. A.; Shimizu, Y. *Appl. Catal., A* **2000**, *200*, 125–134.

(19) Shima, H.; Tatsumi, T.; Kondo, N. *Microporous Mesoporous Mater.* **2010**, *135*, 13–20.

(20) The C═C stretching band of cyclohexene, commonly seen at around 1460 cm^{-1}, was not observed in the infrared spectra due to its low absorption coefficient.

(21) A typical example of the cyclohexane epoxidation with H_2O_2 is as follows: Into a Pyrex reaction vessel were placed catalyst (50 mg), cyclohexane (10 mmol), H_2O_2 (30% aqueous solution, 10 mmol), and acetonitrile (10 mL). The resulting mixture was stirred at 70 °C for 6 h. Cyclohexanol was afforded with >99% selectivity in any case.

(22) (a) Sanderson, R. T. *J. Am. Chem. Soc.* **1983**, *105*, 2259–2261. (b) Mortier, W. J. *J. Catal.* **1978**, *55*, 138–145.

(23) (a) Yamashita, H.; Takada, S.; Hada, M.; Nakatsuji, H.; Anpo, M. *J. Photochem. Photobiol. A* **2003**, *160*, 37–42. (b) Ugliengo, P.; Garrone, E.; Ferrari, A. M.; Zecchina, A.; Otero Areán, C. *J. Phys. Chem. B* **1999**, *103*, 4839–4846.

(24) A $(OH)_3SiOAl(OH)_3$ cluster (referred to as Si(1)Al(1)) was adopted as a zeolite framework model. Full geometry optimizations were performed at the second-order Møller−Plesset perturbation theory (MP2) level. The 6-31G* basis sets were used for H, C, O, Al, Si, Li, Na, and K. The SDD effective core potentials and their basis sets were used for Rb and Cs. The all calculations have been performed with the GAUSSIAN09 suit of programs (Gaussian 09, Revision B.1).

(25) The oxidation of styrene with H_2O_2 was examined as following reaction conditions: Into a Pyrex reaction vessel were placed catalyst (50 mg), styrene (2.5 mmol), H_2O_2 (30% aqueous solution, 1.25 mmol), and acetonitrile (5 mL). The resulting mixture was stirred at 60 °C for 4 h.

(26) [Al,Ti]-MCM-41 (Si/Al = 73 and Si/Ti = 38) was synthesized using cetyltrimethylammonium bromide as a surfactant. Subsequent ion-exchange procedures using CsCl aqueous solution afforded Cs^+@[Al,Ti]-MCM-41 with S_{BET} = 852 m^2/g and V_{total} = 1.16 cm^3/g.